ADVANCED MODELING AND EXPERIMENTAL VALIDATION OF COMPLEX NUCLEAR MATERIAL WASTE FORMS OF POTENTIAL TRANSPORTATION CONCERN

Dan Kelly and Mark T. Paffett
Chemistry Divison
Los Alamos National Laboratory
P. O. Box 1663, Mailstop J565
Los Alamos, NM 87545

ABSTRACT

We present here computer modeling efforts to describe the time-dependent pressurization and gas-phase mole fractions inside sealed canisters containing actinide materials packaged with small (0.12 – 0.5 wt. %) amounts of water. The model is run using Chemkin software, and the chemical reaction mechanism includes gas generation due to radiolysis of adsorbed water, interfacial chemical reactions, and adsorption/desorption kinetics of water on PuO_2 materials. The ultimate goal is to provide a verifiable computer model that can be used to predict problematic gas generation in storage forms and assure design criteria for short-term storage and transportation of less than well-characterized (with respect to gas generation) material classes. Our initial efforts are intended to assess pressurization and gas-phase mole fractions using well-defined 3013 container test cases. We have modeled gas generation on PuO_2 with water loading up to 0.5 wt. %, at 300 and 525 K, for time frames of 3 years. Estimates of the initial H_2 generation rates were determined using RadCalc and employed in the Chemkin model to assess time- and coverage-dependent system behavior. Results indicate that canister pressurization due to radiolysis is a relatively slow process, with pressure increases at 300 K of approximately 1.5 atm. for 5000 g of PuO_2 packaged with 0.5 wt. % water. At higher temperatures (> 400 K), desorption of water into the gas phase largely dictates pressurization and the gas-phase mole fractions. These modeling efforts provide a predictive capability for potential gas generation behavior that when augmented and validated by surveillance information will provide a technical basis for safe storage and transportation.

INTRODUCTION

The potential for radiolytic gas generation to pressurize transportation and storage containers is a major issue affecting the ability of the Department of Energy Environmental Management Program (USDOE-EM) to transport nuclear materials for further disposition (**1**). The current ability to predict canister pressures and gas-phase compositions is restricted by a limited understanding of the fundamental processes that contribute to gas generation. Presently, simple approximations and mathematical models result in a conservatism that is unwarranted for low moisture content actinide oxide materials. This overly conservative approach to predicting gas generation results in significant increased cost for materials management of low moisture content materials. The lack of qualified processes and reliable and validated modeling procedures can lead to expensive testing and frequent delays. The extension of a validated computer model

for gas generation beyond traditional case limits should also be critically examined for potential utility. The scope of our modeling project seeks to extend modeling efforts beyond the simpler cases that incorporate only gas phase reaction chemistry or only radiation derived rates (**2**). Our model includes recombination reactions wherein radiolytically produced hydrogen consumes molecular oxygen, after which the gas-phase mole fraction of hydrogen increases. For short-term storage concerns applicable to transportation scenarios, the inclusion of rates and source terms that drive gas generation are crucial for assuring the integrity of the transported packages. Experimental measurements of $H_2 + O_2$ recombination reactions (which occur at much faster rates than radiolysis events) over pure and impure actinide oxides have unequivocally demonstrated the potential for decreases in canister pressures due to recombination (**3**). In addition, the predilection to create hazardous gas mixtures may be significantly alleviated by this important back reaction. Through leveraging a resource facility at LANL designed to measure gas pressure and composition we will test short-term gas generation changes predicted on the basis of this latest computer model for waste forms most applicable to transportation concerns.

In comparison to common materials and material forms dispositioned as radioactive waste to the Waste Isolation Pilot Plant (WIPP), or other unusual material forms containing transuranic contaminants (e.g., sand slag and crucible materials), a significant fraction of plutonium materials destined to be stored according to DOE Standard 3013-2000 (**1**) are fairly well defined from the standpoint of materials properties. Given this set of initial properties the opportunity to develop a molecular based model that captures all of the known fundamental and empirical knowledge, including thermodynamics and kinetics, concerning interactions of H_2, O_2, and H_2O over PuO_x materials presents a scientific challenge that should prove valuable in assessing safe storage and transportation of these materials. In addition to this fundamental challenge, the concept of predicting long-term behaviors based upon the collective knowledge gained through well designed experiments provides a technical basis to safely store such materials. Aside from the catalytic community where kinetic modeling using molecular-based mechanistic and kinetic rate parameters is a commonly accepted practice, this represents the first use of a molecular-based modeling capability to *a priori* predict and compare the behavior of PuO_2 materials, with specific emphasis on gas generation, sealed in containers under relatively well-defined conditions.

MODEL DESCRIPTION

Our model has been developed using Chemkin (**4**) software (Reaction Design). Chemkin provides a modular format where chemical equations describing gas-phase and heterogeneous reaction mechanisms are evaluated and subsequently linked to an application program. We are evaluating the chemistry occurring in sealed canisters using the Aurora application module, which simulates a constant stirred tank reactor. We run Aurora in a closed-system transient mode to determine canister pressure and gas-phase mole fractions as a function of time.

Shown in Table 1 is the reaction mechanism we have developed to globally describe the pertinent reactions occurring in sealed PuO_2 systems. Our current reaction mechanism of eleven equations includes radiolysis, interfacial chemical reactions, and

water adsorption/desorption kinetics that contribute to gas generation. The work to date has employed clean plutonium oxide surfaces with little or no attention to the influence of impurities or reactions at container surfaces. Most of these modeling mechanisms require refinement and modification to reflect continuing experimental and theoretical investigation of the reactions they describe. As an example, the radiolytic production of hydrogen peroxide follows from experiments in liquid water and may have limited utility in low moisture content modeling scenarios (**5, 6**). In addition, the production of hydrogen peroxide may not occur on plutonium oxide surfaces. Also, we are aware that radiolysis of gas-phase constituents may lead to recombination of hydrogen and oxygen to form water (**5**), however, we believe the rate of chemical recombination (undoubtedly through a surface-mediated mechanism not detailed here) is much faster (**3**).

Table I: Global reaction mechanism for gas generation on PuO_2, where the rate coefficient for reaction, k, is equal to $A * T^{\beta} * \exp(-E_a/RT)$.

#	Radiolytic Reactions	A (mol/sec^{-1})	β	E_a (kcal/mol)
1	$H_2O_{(s)} \Rightarrow \frac{1}{2} H_{2(g)} + \frac{1}{2} H_2O_2$	8.33×10^{-9}	0	0
2	$PuO(OH)_2 \Rightarrow PuO_2 + \frac{1}{2} H_{2(g)} + \frac{1}{2} H_2O_2$	8.33×10^{-9}	0	0
3	$H_2O_2 \Rightarrow H_2O_{(g)} + \frac{1}{2} O_{2(g)}$	8.33×10^{-9}	0	0
	Chemical Reactions			
4	$H_{2(g)} + \frac{1}{2} O_{2(g)} \Rightarrow H_2O_{(g)}$	4.9×10^{-4}	0	0
5	$H_2O_{(g)} \Rightarrow H_2O_{(s)}$	0.2[(a)]	0	0
6	$H_2O_{(s)} \Rightarrow H_2O_{(g)}$	1×10^{13}	0	10.5[(b)]
7	$H_2O_{(s)} + PuO_2 \Rightarrow PuO(OH)_2$	8.1×10^{-4}	0	0
8	$PuO(OH)_2 \Rightarrow PuO_2 + H_2O_{(s)}$	5.6×10^{-1}	-1	30.7
9	$PuO(OH)_2 + \frac{1}{2} O_{2(g)} \Rightarrow PuO_2(OH)_2$	4.4×10^{-6}	0	9.4
10	$PuO(OH)_2 + H_2O_2 \Rightarrow PuO_2(OH)_2 + H_2O_{(s)}$	4.4×10^{-6}	0	9.4
11	$PuO_2(OH)_2 + H_{2(g)} \Rightarrow PuO(OH)_2 + H_2O_{(s)}$	8.85×10^{-10}	1	0

[(a)] Sticking Coefficient

[(b)] $E_{a\ (300\ K)} = 10.5$, $E_{a\ (525\ K)} = 8.4$

Values in Table I are provided on a molar basis to evaluate the reaction rate coefficient for each reaction, given as:

$$k = A * T^{E} * \exp(-E_a/RT). \qquad \text{(Eq. 1)}$$

Chemkin solves the set of gas-phase and heterogeneous reaction equations simultaneously and evaluates overall reaction rates according to a concentration-dependent expression. For example, the rate of surface reactions such as the radiolysis of adsorbed water to form peroxide and gas-phase hydrogen (Reaction 1) is given by

$$\text{rate} = k * Y * SA * [H_2O], \qquad \text{(Eq. 2)}$$

where ρ is the PuO_2 surface site density (moles/cm^2), SA is the total PuO_2 site area (cm^2), and $[H_2O]$ is the concentration, or fractional coverage, of adsorbed water. It should be noted that all of the above reaction equations are evaluated as pseudo-first order reactions, and the reaction rates are simply dependent on the concentration of reactant species. Empirical molar kinetic rate values for the pre-exponential term of Eq. 1 are supplied for the majority of the reactions in Table I because experimentally derived rate coefficients for reactions similar to those found here are most often expressed as molar rates. Values to describe the adsorption/desorption behavior of water use a sticking coefficient for water adsorption, while water desorption employs a first-order frequency factor (10^{13}) and activation energy equal to the enthalpy of desorption at the simulation temperature. We have verified that these kinetic values regarding water reliably reproduce experimentally determined pressure vs. temperature curves during the adsorption/desorption of water on PuO_2 as temperature is cycled from 295 to 530 K and returned to 295 K (**7**). Rate coefficients for Reactions 7-11 have been derived from experimental reports investigating the interactions of water and PuO_2 systems (**8-13**). We note that the rate of these PuO_2 surface reactions in our model have at most a minor effect on the canister pressurization and gas-phase content.

The preexponential terms of Table I to describe radiolysis events (Reactions 1-3) have been chosen such that the initial (time = 0) rate of hydrogen production by radiolysis of adsorbed water predicted by the Chemkin model matches that predicted by RadCalc. RadCalc predicts (**2**) a molar rate of hydrogen production of approximately 7 x 10^{-9} moles/sec, using an input of 5000 g PuO_2 (designated as pure Pu-239) and 25 g, or 0.5 wt. %, water. Note that these rates can be easily calculated to reflect a different isotopic fraction in the starting material. For the surface area and site density used to depict 5000 g PuO_2 in the Chemkin model, a rate coefficient of 8.33 x 10^{-9} moles/sec gives an initial gas generation rate of 7 x 10^{-9} moles H_2/sec arising from the radiolysis of 25 g of adsorbed water. We note that RadCalc does not conserve mass and hence predicts a constant rate of H_2 production (for constant loadings of PuO_2 and H_2O), no matter what fraction of the initially loaded water is extant in the system over time. Chemkin, however, accounts for the fact that as radiolysis of water proceeds, the rate of hydrogen production must decrease because the concentration of water is diminishing. As a first approximation to describing the overall behavior of the gas generation system, we have chosen identical rate coefficients for all radiolytic reactions. Undoubtedly, Reactions 2 and 3 will have rates that differ from Reaction 1, however, as shown below it is the rate of Reaction 1 that predominantly drives the gas generation rate in our model, especially with water loadings greater than 1 monolayer (ML). There is much controversy regarding rates for oxygen production through the radiolysis of water, or radiolysis rates for first layer hydroxyls, that is esoteric to the general results shown

below. These rates can be modified as new results emerge from collaborative experimental programs.

Other pertinent simulation parameters and methodology are as follows. DOE Standard 3013 (**1**) dictates that the maximum loading of actinide oxide material in sealed canisters is 5000 g, and the maximum allowable loading of water is 0.5 wt. %, or 25 g H_2O. We consider the canister in our simulations to have the dimensions of an "inner" can, with a volume of 2266 ml. In all simulations the canister is portrayed to contain 5000 g PuO_2 with a density of 11.5 g/ml, and hence the free volume of the can is 1831 ml. A surface area of 5 m^2/g is assumed for the PuO_2. Assuming a site area for water adsorption of 12.5 $Å^2$, we note that 0.5 wt. % H_2O corresponds to a surface coverage of 4.2 ML of H_2O on 5000 g of PuO_2. In all cases the canister is packaged with dry air (21 % O_2, 79 % N_2) at 300 K and 1 atm. Simulation times presented here are 3 years, although longer time simulations are easily accommodated. Simulations at temperatures higher than 300 K are carried out by ramping the system to the desired temperature over a short time period (~ hours) within the 3-year simulation time frame. The change in pressure accompanying this temperature change is accounted for by the ideal gas law, i.e., a simulation at 525 K has an effective initial pressure of (525 K / 300 K) * 1 atm. = 1.75 atm., as it should since it is packaged at 300 K and 1 atm.

Our model allows for chemical reaction rates that are dependent on water loading. Since relatively small mass loadings of water (~ 0.5 wt %) correspond to multiple layers of adsorbed water on PuO_2, the ability to incorporate concentration-dependent water reactions into the model may be paramount to properly describing the overall system behavior. Specifically, experimental evidence suggests that the radiolysis rate coefficients for adsorbed water are dependent on the proximity of the water to the radiolytic source (**14**). Hence, proper description of the behavior for a 0.5 wt % water loading may require the rate coefficient of water radiolysis of the fourth ML to be substantially different than that of first ML water directly bound to the PuO_2 surface. We note that only reactions involving the radiolysis of water (Reaction 1), and the radiolysis of subsequently formed peroxides (Reaction 3), are affected by this layering approach. Reactions involving PuO_2 moieties and water occur only within the first water ML and hence their rate expressions would not be expected to be dependent on the amount of water present. Also, we find that Reactions 5 and 6 describing water adsorption/desorption are adequate to qualitatively reproduce experimental H_2O thermal desorption results on PuO_2 surfaces for water loadings corresponding to at least 10 ML (**7**). This methodology of correlating the mass of water loaded to a layered simulation structure where the kinetic parameters describing water reactions are layer-dependent is referred to several times below and the layer-dependent radiolysis rates are delineated where necessary.

RESULTS

Shown in Fig. 1 is a plot of canister pressure vs. time at 300 K for 5000 g PuO_2 packaged with 0.5 wt. % H_2O, determined using several modeling methods. Trace 1(a) shows the linear pressure rise predicted by RadCalc due to H_2 generation through the radiolysis of water. Trace 1(b) shows the pressure rise predicted by Chemkin-Aurora, provided only radiolysis of water to form gas-phase H_2 and adsorbed H_2O_2 occurs (Reaction 1 from Table I). A rate coefficient of 8.33×10^{-9} moles/sec has been employed

here to give the same initial H_2 production rate as predicted by RadCalc. Also, the entirety of the H_2O is assumed to undergo radiolysis with the same rate coefficient. Although 0.5 wt. % corresponds to over 4 ML of water, in trace 1(b) there is no dependence of the radiolysis rate on which ML the water resides. Trace 1(c) depicts canister pressurization due to H_2 generation from radiolysis of water, predicted by Chemkin-Aurora. As in trace 1(b), only reaction 1 of the model is operative, but now the radiolysis rate depends on which layer the water resides. Experimental results indicate that the radiolysis rate of water depends on how close the water is located to the radiolytic source, with rates dropping as the water is located further from the source (**14**). In 1(c) the rate coefficient for radiolysis of each successive water layer is halved from that of the previous layer, and just over 4 layers are used to account for the 0.5 wt % loaded. Trace 1(d) shows the pressure predicted by Chemkin-Aurora for the full model (all 11 reactions) of Table I. Although the initial radiolytically-driven hydrogen production rate in 1(d) is equal to that of 1(c), an initial pressure decrease is observed when the full model is employed. This arises because the rate of recombination of H_2 and O_2 to reform water initially decreases the pressure of the canister. When oxygen has been removed from the gas phase the canister pressure rises due to H_2 generation by radiolysis. The removal of oxygen from the gas phase has been observed experimentally from studies of sealed PuO_2 systems, presumably because of this recombination reaction (**3**). The dominance of the recombination reaction in Table I dictates that oxygen is removed at approximately the same rate that H_2 is generated by radiolysis.

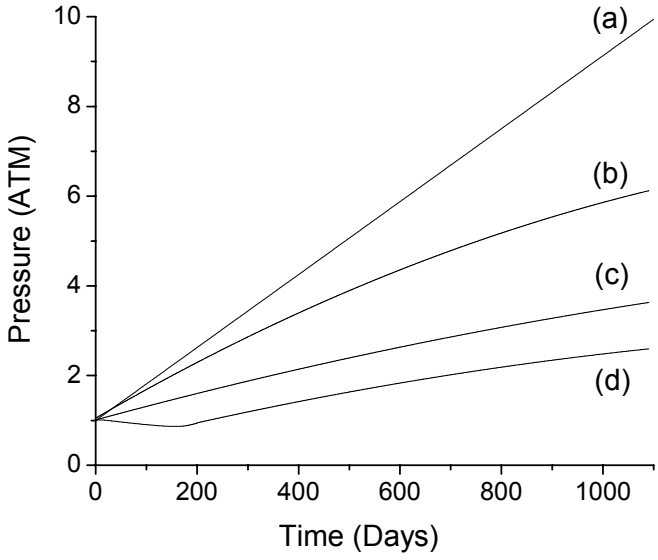

Fig. 1: Canister pressure vs. time at 300 K for a number of modeling scenarios; (a) RadCalc; (b) Chemkin single-layer radiolysis; (c) Chemkin multi-layer radiolysis; (d) Chemkin model of Table I. See text for further explanation.

Shown in Fig. 2 is a plot of canister pressure vs. time for 5000 g PuO_2 at 300 K and packaged with water loadings of 0.12 to 0.5 wt. %, corresponding to surface coverages of 1 to 4.2 ML. In this, and all subsequent figures, plots have been generated

using the full global model of Table I, with initial (first ML) radiolysis rate coefficient determined using RadCalc as described above. Also, for this and subsequent figures, radiolysis rate coefficients for each successive ML of water loaded are equal to half the previous ML, identical to the description for trace 1(d) above. As expected, increasing the water loading leads to increased final pressures at the end of the 3-year simulation time frame. With increasing water loading the overall rate of H_2 generation increases, though in a non-linear fashion since the rate coefficients for radiolysis are halved for each successive ML of water loaded. The initial periods of decreasing pressure correspond to oxygen removal from the gas phase due to recombination with radiolytically produced hydrogen. The rate of hydrogen production from radiolysis increases as water loading increases, the result being shorter times required to remove oxygen from the gas phase. After oxygen removal from the gas phase, pressures increase due to generation and buildup of hydrogen from water radiolysis, the rate being dependent on water concentration and increasing with increasing water loading.

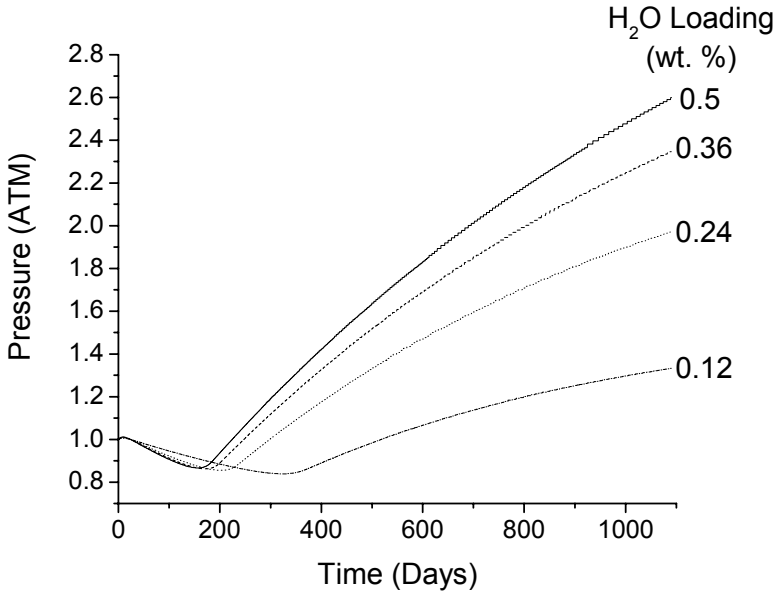

Fig. 2: Canister pressure vs. time for water loadings of 0.12 to 0.5 wt. % at 300 K, determined using the model shown in Table I.

Shown in Fig. 3 is a plot of the gas-phase mole fraction of oxygen and hydrogen for water loadings of 0.12 and 0.5 wt. % and a temperature of 300 K. These traces depict the experimental observation that the gas-phase concentration of hydrogen remains relatively low while oxygen is present. Also, the depletion of oxygen from the gas phase occurs with approximately a constant rate vs. time, dependent on initial water loading. Since the rate of recombination of oxygen and hydrogen to reform water is appreciably faster than the rate of hydrogen generation from water radiolysis, the oxygen depletion rate approximately mimics the hydrogen generation rate. The hydrogen generation rate increases with increasing water loading. The hydrogen production rate remains approximately constant for a specific water loading while oxygen is present because

hydrogen and oxygen recombine to restore the supply of adsorbed water. Once oxygen is removed the concentration of hydrogen rapidly increases, slowing only when the surface concentration of water substantially drops.

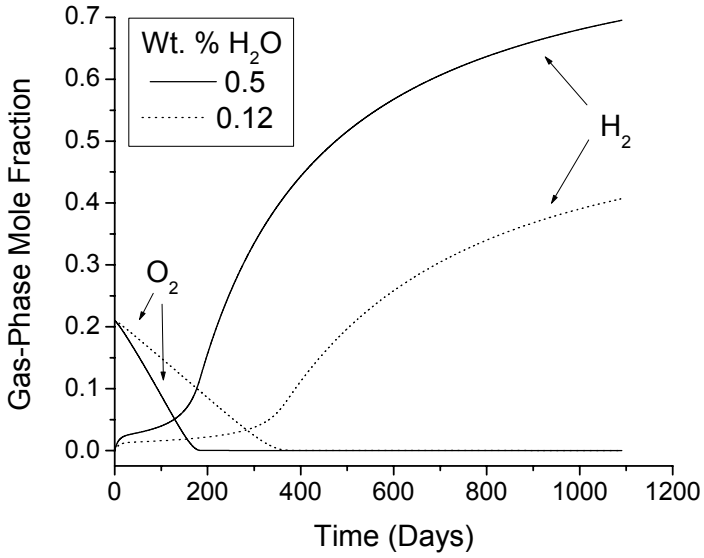

Fig. 3: Gas-phase mole fraction of H_2 and O_2 vs. time for water loadings of 0.12 and 0.5 wt. % at 300 K, determined using the full model of Table I.

Shown in Fig. 4 is a plot of canister pressure vs. time at 525 K for water loadings of 0.12 to 0.5 wt. %. At this temperature multilayer water rapidly desorbs from the PuO_2 surface. The primary source of hydrogen gas generation arises from the radiolysis of tightly bound hydroxyl and peroxide moieties generated from the chemical decomposition of water on PuO_2 sites. The desorption of water, as well as the increase in system temperature from 300 to 525 K, lead to rapid substantial pressure increases. However, the rate of hydrogen generation is relatively constant with water loading since most of the water is in the gas phase and unavailable for radiolysis to form H_2. After the immediate pressure rise, canister pressure slowly decreases approximately 0.2 atm. due to removal of oxygen through recombination with hydrogen to form water. Even at this high temperature both the initially desorbed water and reformed water may adsorb on bare PuO_2 sites and dissociatively react to form adsorbed hydroxyls or radiolyze to form hydrogen and adsorbed peroxides. However, over the time frame of the simulation, the concentration of bare PuO_2 sites is never appreciable and subsequent reactions of desorbed water are negligible.

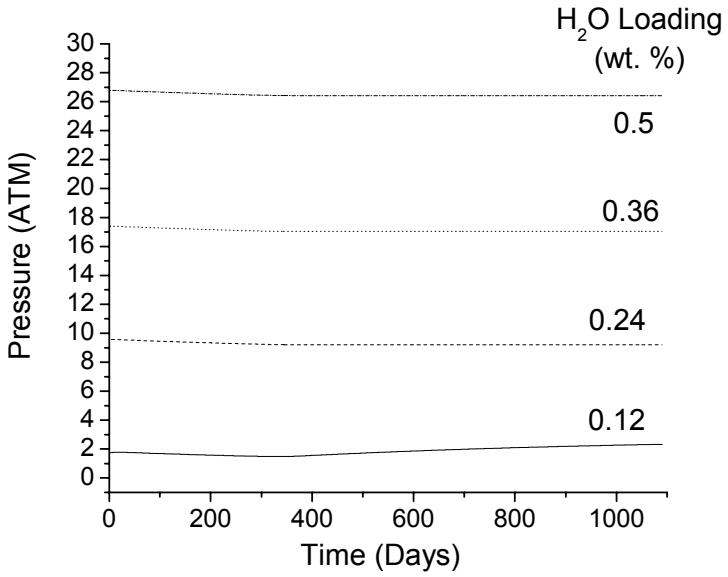

Fig. 4: Canister pressure vs. time at 525 K for water loadings of 0.12 to 0.5 wt. %, determined using the full model of Table I.

Shown in Fig. 5 is the gas-phase mole fraction of hydrogen vs. time at 525 K for water loadings of 0.12 to 0.5 wt. % (1 to 4.2 ML). The hydrogen concentration reaches substantial levels (> 10 %) only for a 1 ML water loading. According to the mechanism of Table I, the first ML of water facilely dissociates to form tightly bound hydroxyls on PuO_2. These hydroxyls may undergo radiolysis to form hydrogen that accumulates in the gas phase after depletion of the oxygen. Loading multilayer amounts (> 1 ML or 0.12 wt. %) of water results in water desorption at 525 K. Not only is the desorbed water unavailable for the generation of hydrogen by radiolysis, but the large amount of water in the gas phase leads to a decrease in the gas-phase hydrogen mole fraction. However, the rate of hydrogen generation, and hence absolute moles of hydrogen in the gas phase, in each of the traces of Fig. 5 is approximately constant since the first ML of water is tightly bound and undergoing radiolysis.

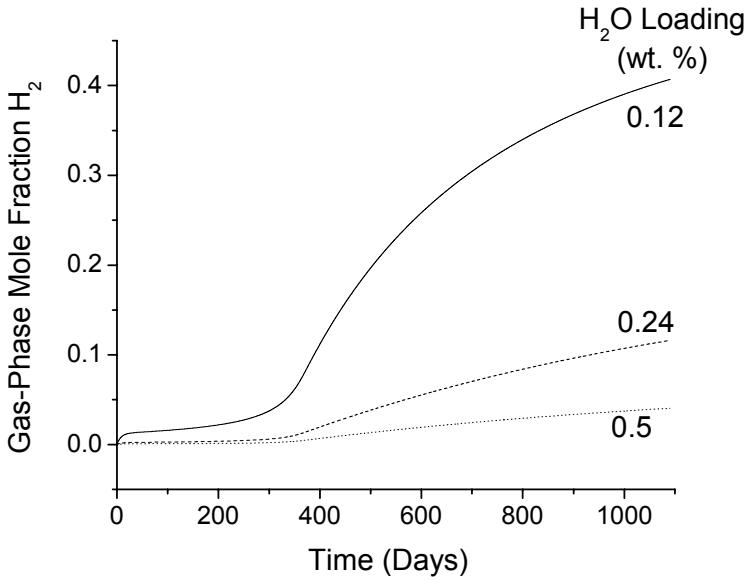

Fig. 5: Gas-phase mole fraction of H_2 vs. time for water loadings of 0.12 to 0.5 wt. % at 525 K, determined using the full model of Table I.

CONCLUSIONS

A computer modeling effort has been developed to simulate the chemistry occurring in sealed canisters containing PuO_2 and water. A global reaction mechanism including radiolysis of adsorbed OH species, interfacial chemical reactions, and water adsorption/desorption kinetics is used. Reaction rate coefficients for radiolysis events are determined using RadCalc. Rate coefficients for interfacial reactions, water adsorption/desorption, and the gas-phase recombination of hydrogen and oxygen to form water are taken from the experimental literature. Results indicate that at room temperature, radiolysis of water to form gas-phase hydrogen is the dominant gas generation process leading to canister pressurization. The fast recombination of oxygen and hydrogen to reform water depletes oxygen from the gas phase prior to appreciable buildup of hydrogen, and leads to an initial pressure decrease in the canister. Upon complete removal of oxygen from the gas phase, hydrogen generation leads to increasing canister pressures. However, at room temperature the pressure achieved for 5 kg PuO_2 packaged with 0.5 wt. % H_2O is only approximately 2.5 atm. after 3 years. At high temperature (525 K), desorption of water is rapid and leads to substantially higher pressures than observed at room temperature, for a given water loading. Also at high temperature, the mole fractions of gas-phase constituents are substantially dependent on water loading due to the predilection of water to desorb and the predominance of water in the gas phase. Future efforts will be aimed at model validation using gas generation data collected in controlled experiments.

ACKNOWLEDGMENT

Primary support for this investigation was made possible by the Department of Energy's Nuclear Materials Focus Area and the Nuclear Materials Stabilization Program Office, United States Department of Energy, Albuquerque Operations and Headquarters Offices, under the auspices of the DNFSB 94-1 Research and Development Project.

REFERENCES

1. DOE Standard 3013-2000, "Stabilization, Packaging and Storgae of Plutonium Bearing Materials", US Dept. of Energy. 2000.
2. J. G. McFadden, Radcalc for Windows Version 2.01, Volume 1: User's Manual, HNF-2549, Rev. 0, 1995.
3. L. A. Morales, "Preliminary Report on the Recombination Rates of Hydrogen and Oxygen over Pure and Impure Plutonium Oxides," Report LA-UR-98-5200, Los Alamos National Laboratory, Los Alamos, NM, 1998.
4. R. J. Kee, *et. al*., *Chemkin Collection*, Release 3.6, Reaction Design, Inc., San Diego, CA, 2000.
5. J. Spinks and R. J. Wood, *An Introduction to Radiation Chemistry,* John Wiley & Sons, Inc., New York, 1990.
6. A.A. Garibov, "Water Radiolysis in the Presence of Oxide," In: *Proceedings of the Fifth Tihany Symposium on Radiation Chemistry Held at Siofok 19-24 September 1982. Vol. 1, 2,* Hungary Akademiai Kiado, Budapest, 377, 1983.
7. M. T. Paffett, D. Kelly, and K. Veirs, J. Nucl. Mat., submitted.
8. J. M. Haschke and T. H. Allen, "Interactions of Plutonium Dioxide and Water and Oxygen-Hygrogen Mixtures,", LA-13537-MS, January 1999.
9. J. Haschke, "Reactions of Plutonium and Uranium with Water: Kinetics and Potential Hazards,", LA-13069-MS, December 1995.
10. J. Stakebake, J. Phys. Chem., 77 (1973) 581.
11. L. A. Morales, J. M. Haschke, and T. H. Allen, "Kinetics of Reaction Between Plutonium Dioxide and Water at 25^{o}C to 350^{o}C: Formation and Properties of the PuO_{2+x} Phase," Report LA-13597-MS, Los Alamos National Laboratory, Los Alamos, NM, May 1999.
12. J. M. Haschke, T. H. Allen, and J. L. Stakebacke, J. Alloys Comp., **243** (1996) 23.
13. J. M. Haschke and T. E. Ricketts, J. Alloys Comp., **252** (1997).
14. J.A. LaVerne and L. Tandon, J. Phys. Chem. B 106 (2002) 380-386.